Experimental Evaluation of 3D Geoelectrical Resistivity Imaging using Orthogonal 2D Profiles

A. P. Aizebeokhai[1]*, A. I. Olayinka[2], V. S. Singh[3] and O. A. Oyebanjo[4]
[1]Department of Physics, Covenant University, Ota, Nigeria, philips_a_aizebeokhai@yahoo.co.uk;
[2]Department of Geology, University of Ibadan, Ibadan, Nigeria, aiolayinka@yahoo.com;
[3]National Geophysical Research Institute, Hyderabad, India, vssingh77@hotmail.com
[4]Department of Physics/Telecommunication, Tai Solarin University of Education, Ijagun, Nigeria

ABSTRACT

Numerical evaluation of 3D geoelectrical resistivity imaging was conducted using orthogonal set of 2D pseudo-sections generated over two synthetic models, horst and trough models. The models represent geological environment that simulates a typical weathered profile and refuse dump site in a crystalline basement complex, respectively. Different arrays including Wenner-alpha (WA), Wenner-beta (WB), Wenner-Schlumberger (WSC), dipole-dipole (DDP), pole-dipole (PDP), and pole-pole (PP) arrays were used for the data generation. The 2D apparent resistivity data were collated to 3D data set and then inverted using a full 3D inversion code. The effectiveness of the technique for 3D resistivity imaging as well as the imaging capabilities of the selected arrays is evaluated. The observed anomaly effect and normalized model sensitivities of the arrays indicate that DDP and PDP arrays are more sensitive to the 3D features, while WSC show moderate sensitivity to 3D features. Field example in which the technique was applied in a 3D geoelectrical resistivity imaging for engineering site investigation in the crystalline basement complex of southwestern Nigeria is also presented.

Keywords: 3D Imaging, Resistivity Surveys, Orthogonal Profiles, Environmental Investigations

INTRODUCTION

Geoelectrical resistivity imaging has been used to address hydrological, environmental and geotechnical issues. Conventional vertical electrical sounding is inadequate to map subsurface with complex and multi-scale geology often encountered in environmental and engineering investigations. Two-dimensional (2D) resistivity imaging has been widely used to map areas with moderately complex geology (e.g. Griffiths and Barker, 1993; Dahlin and Loke, 1998; Amidu and Olayinka, 2006; Aizebeokhai et al., 2010). But geological structures and subsurface petrophysical properties are inherently three-dimensional; hence the 2D resistivity imaging often produce out-of plane anomaly which could be misleading in the interpretation of subsurface features (Bentley and Gharibi, 2004). Thus, a three-dimensional (3D) model of interpretation which allows resistivity variation in all possible directions should give a more accurate and reliable inverse resistivity models of the subsurface.

In ideal 3D survey, data measurements that constitute a complete 3D data set are made in all possible directions (Loke and Barker, 1996a; Aizebeokhai, 2010). Pole-pole (e.g. Loke and Barker, 1996a) and pole-dipole (e.g. Chambers et al., 1999) arrays are reported to more suitable for this multi-directional data collection. Square or rectangular grid of electrodes with constant spacing in both x- and y-directions, in which each electrode is in turn used as current electrode and the potential measured at all other electrode positions, are commonly used. But the ideal 3D surveying technique is usually impractical due to the site geometry, length of cables, number of electrodes and electrode spacing involved in practical 3D resistivity surveys. Also, the surveying technique is time consuming in surveys involving large grid. A cross-diagonal surveying technique (Loke and Barker, 1996a), in which measurements are made along the x-axis, y-axis and 45-degrees diagonal lines, can be used to reduced the time and effort required for the survey. However, this technique still involves large number of independent measurements for medium to large grids. Alternative techniques, which allow flexible survey design, choice of array and easy adaptability to data acquisition systems, involve the combination parallel 2D lines (e.g. Chambers et al., 2002) or orthogonal 2D lines (e.g. Aizebeokhai et al., 2009; 2010) to construct 3D images.

Traditionally, the imaging capability of different arrays differs for different geological structures. In this paper, Wenner-alpha (WA), Wenner-beta (WB), Wenner-Schlumberger (WSC), dipole-dipole (DDP), pole-dipole (PDP) and pole-pole (PP) arrays were used to generate apparent resistivity data for a set of orthogonal 2D lines over two synthetic models. The relative effectiveness and imaging capabilities of the orthogonal set of 2D profiles for 3D geoelectrical resistivity survey were evaluated. The responses of these models to 3D inversion for the different arrays are assessed using the normalized average model sensitivity values and the 3D inverse models. Differences in the arrays spatial resolution are evaluated. Field example in which the technique was applied in a 3D geoelectrical resistivity imaging for engineering site investigation in the crystalline basement complex of southwestern Nigeria is also presented.

METHODS OF STUDY

Two synthetic model geometries (Figure 1) were designed to simulate a typical weathered profile and refuse dump site usually associated with geophysical applications to environmental and engineering investigations in tropical crystalline basement complex (Aizebeokhai et al., 2009). The horst structure consists of a three layers model comprising of the top soil, saprolite (the weathered zone) and the fresh basement with varying resistivities and thicknesses. Similarly, the trough model consist of three layers in which the top and the middle layer vary in thickness with a maximum of 4.2 m and 11.8 m, respectively, and the underlying third layer is a basement rock of infinite thickness. The trough structure is assumed to be at the centre of the model with varying lateral thickness and cutting across the first and second layers.

The 3D synthetic models were approximated into series of 2D models separated with a constant interval in both parallel and perpendicular directions. Apparent resistivity data were calculated over the resulting orthogonal 2D profiles for the selected arrays. Electrode layouts with different minimum separations, a and inter-line spacing, L (a = 2 m, 4 m, 5 m and 10 m; L = a, 2a, 2.5a, 4a, 5a and 10a) were used in the calculation of the apparent resistivity data. The 2D modelling accounts for 3D effect of current sources; thus the resistivity of each of the model was allowed to vary arbitrarily along the profile and with depth, but with an infinite perpendicular extension. Finite difference method (Dey and Morrison, 1979), which determines the potentials at the nodes of the rectangular mesh, was employed in the calculation of the potential distribution. The calculated apparent resistivity values were contaminated with 5% Gaussian noise (Press et al., 1996) so as to simulate field conditions.

The apparent resistivity data computed for the series of 2D models were collated to 3D data set using RES2DINV inversion software (Loke and Barker, 1996b). The number of electrodes in each 2D profile, number of profiles collated and their directions determine the size and pattern of the electrode grid obtained of the 3D data set. The collated 3D data sets were inverted using RES3DINV computer code (Li and Oldenburg, 1994). The inversion routine is based on the smoothness constrained least-squares method (de Groot-Hedlin and Constable, 1990).

RESULTS AND DISCUSSIONS

The 3D inverse models for the arrays considered were carefully examined. The horizontal depth slices of the 3D inverse models for the grid size of 21x21 and inter-line spacing of $4a$ for the host structure are presented in Figure 2 as representatives. Similar images are obtained for the trough model. The horizontal depth slices show lateral and vertical variations in the inverse models depicting the subsurface features. The thickness of the horizontal depth slices generally increases with depth and varies from array to array, depending on the electrode spacing used for the survey. The 3D images produced from the orthogonal set of 2D profiles do not show grid orientation effects commonly observed if only parallel 2D profiles are used.

The imaging capabilities of the arrays are different for the same survey parameters when applied to a particular geologic structure. These differences are often reflected in the spatial resolution, tendency to produce artefacts, deviations of the inverse resistivity models from the true resistivity models and the effective depth of investigations. Resolution is a complex function of numerous factors (such as electrode layout, data quality, imaging or inversion algorithm, and electrical conductivity distribution) and generally varies significantly across the image plane. To obtain reliable and high resolution inverse models, the array should ideally give data with maximum anomaly information, reasonable data coverage and high signal-to-noise ratio. A complete data set with minimum noise contamination is therefore required for such a high resolution inverse models. But acquiring such data set would significantly increase the time required for the survey. A large data set points could also makes it difficult for the inversion to attain a good data misfit due to the unknown characteristics of the noise contamination in the data.

The sensitivity pattern of an array is an important factor in the determination of its imaging capability. The sensitivity analyses shows that for the combinations of orthogonal set of 2D profiles, the DDP, PDP and WSC arrays are more sensitive, while PP, WA and WB arrays are the least sensitive arrays to 3D features. However, the more sensitive arrays have the least effective depth of penetration. The normalised average model sensitivities observed in the 3D inverse models obtained from the inversion of the various data sets for the selected arrays with different electrode grid sizes and inter-line spacing are presented in Table 1. The observed average model sensitivity and hence the image resolution increases with increasing data density and decreasing inter-line spacing. In general, the overall sensitivity of the image plane decreases rapidly with depth, indicating significant loss of resolution with depth. Thus, arrays with high effective depth of penetration yields low average model sensitivity.

The inter-line spacing between the orthogonal 2D profiles to be combined into 3D data set should be the same with the minimum electrode spacing. This would yield uniform electrode grids and reduced sparceness of the data set and thus produce good quality and high resolution images. But this is not often achievable in practice. A qualitative analysis of the inversion images and their corresponding sensitivity maps obtained from both smootness constrained inversion methods show

that inter-line spacing of less or equal to $4a$, a being the minimum electrode spacing, would yield good quality and high resolution 3D images. However, inter-line spacing greater than this can give resonable resolution but may contain more near-surface actefacts. Thus, inter-line space greater than $4a$ could be used if the near-surface feactures are not the main features of interest. The RMS error in the inversion models is relatively higher than those obtained when convention square grids are used. This is becuse the 2D profiles combined to form 3D data set consist of different error characteristics. The RMS error in inversion decreases with decreasing inter-line spacing relative to the minimum electrode separation.

FIELD EXAMPLE

Orthogonal set of 2D resistivity field data, consisting of six parallel and five perpendicular profiles, were collected in an investigation site using WA array. Seven vertical electrical soundings were also conducted on the site to provide ID layering information and supplement the orthogonal 2D profiles. The site, underlain by crystalline basement complex rocks, is located within the University of Ibadan, southwestern Nigeria. The dominant rock types are quartzites of the meta-sedimentary series and banded gneisses, augen gneisses and migmatites which constitute the gneiss-migmatite complex. The survey was to determine the degree of weathering and fracturing in the weathered profile, and ascertains the suitability of the site for engineering constructions as well as determining its groundwater potential. The 2D apparent resistivity data were processed separately and then collated into 3D data set which was inverted using a 3D inversion code. The 3D inverse models obtained are presented as horizontal depth slices in Figure 3. The 3D inversion images increased the degree of reliability of the geoelectrical resistivity imaging. Unrealistic artefacts and spurious features due to 3D effects commonly associated with 2D inversion images are minimized or completely eliminated in the 3D inversion images.

Table 1: Average model sensitivities for the 3D inverse models: a) horst model and b) trough model

a)

Array	**Average Sensitivity**							
	11 x 11 $L = a$	11 x 11 $L = 2a$	21 x 21 $L = 2a$	21 x 21 $L = 4a$	26 x 26 $L = 5a$	31 x 31 $L = 2.5a$	51 x 51 $L = 5a$	51 x 51 $L = 10a$
WA	-	-	1.0141	0.5532	0.4793	0.7434	0.6963	0.3840
WB	-	-	0.8824	0.4766	0.4040	0.6432	0.7060	0.5070
WSC	2.0578	1.1254	1.8978	1.0313	0.9116	1.3774	1.3156	0.7123
DDP	3.7586	2.0559	2.7118	1.4650	1.8526	2.7871	3.6277	1.9687
PDP	3.4507	1.8852	2.7242	1.4758	1.4525	2.2134	2.6987	1.4682
PP	1.6864	0.9332	0.9990	0.5413	0.4801	0.4387	0.6234	0.3374

b)

Array	**Average Sensitivity**							
	11 x 11 $L = a$	11 x 11 $L = 2a$	21 x 21 $L = 2a$	21 x 21 $L = 4a$	26 x 26 $L = 5a$	31 x 31 $L = 2.5a$	51 x 51 $L = 5a$	51 x 51 $L = 10a$
WA	-	-	1.0340	0.5636	0.5492	0.4799	0.6485	0.3585
WB	-	-	0.9064	0.7383	0.5127	0.5011	0.6464	0.4155
WSC	1.9585	1.0691	1.8419	1.0010	1.0150	0.8814	1.2760	0.7065
DDP	3.7221	2.0282	2.6946	1.4749	1.8683	1.5581	2.5335	1.3121
PDP	3.3673	1.8288	2.6986	1.4627	1.4354	1.4524	1.8457	0.9794
PP	1.4140	0.8152	0.7349	0.4282	0.3735	0.3354	0.4212	0.2587

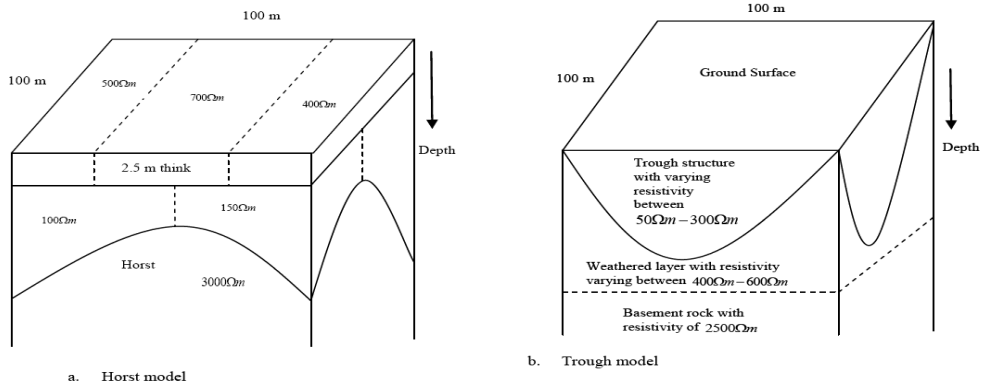

Fig. 1: Synthetic models: (a) horst model simulating a typical weathered profile above, and (b) trough model simulating waste dump site (after Aizebeokhai et al., 2009; Aizebeokhai and Olayinka, 2010) in crystalline basement complex.

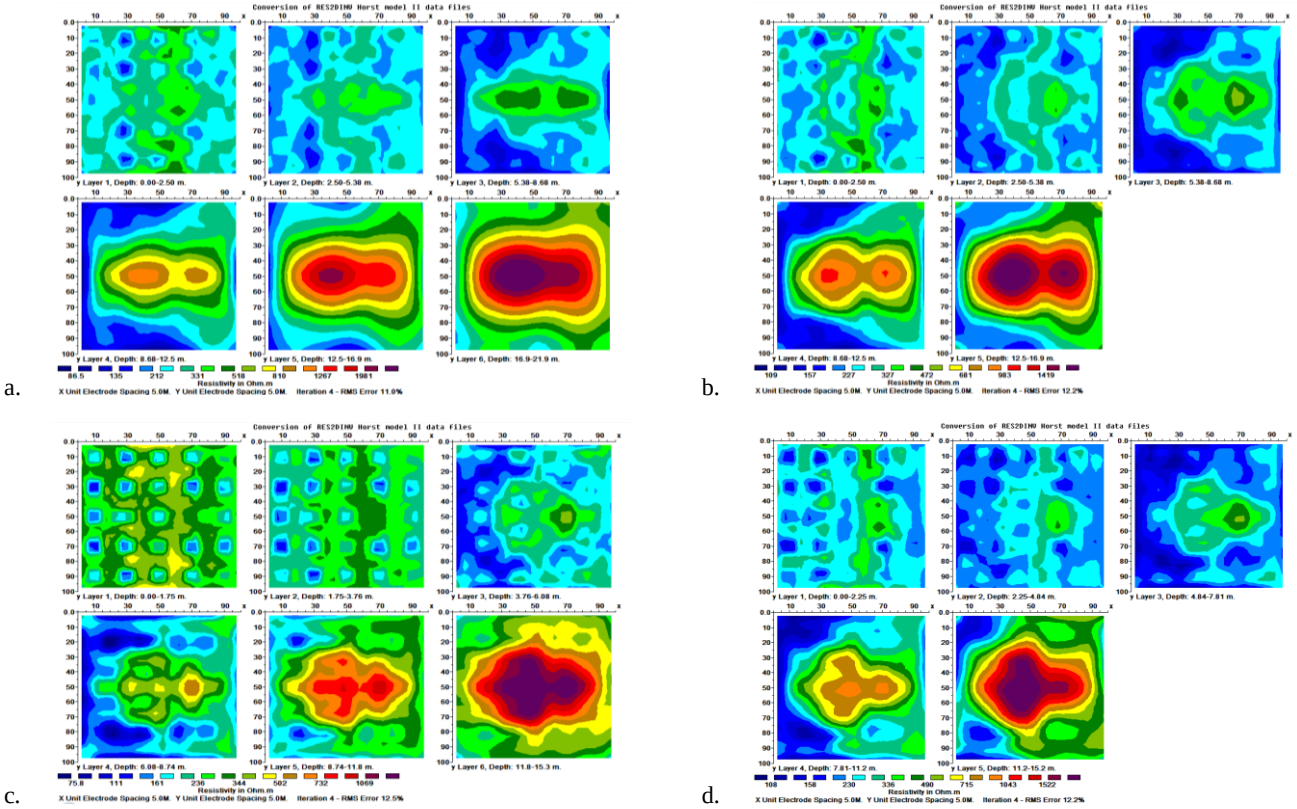

Figure 2: Inverse model for horst model structure with grid size of 21x21 and inter-line spacing of $4a$: a) Wenner-alpha, b) Wenner-Schlumberger, c) dipole-dipole and d) pole-pedipole arrays.

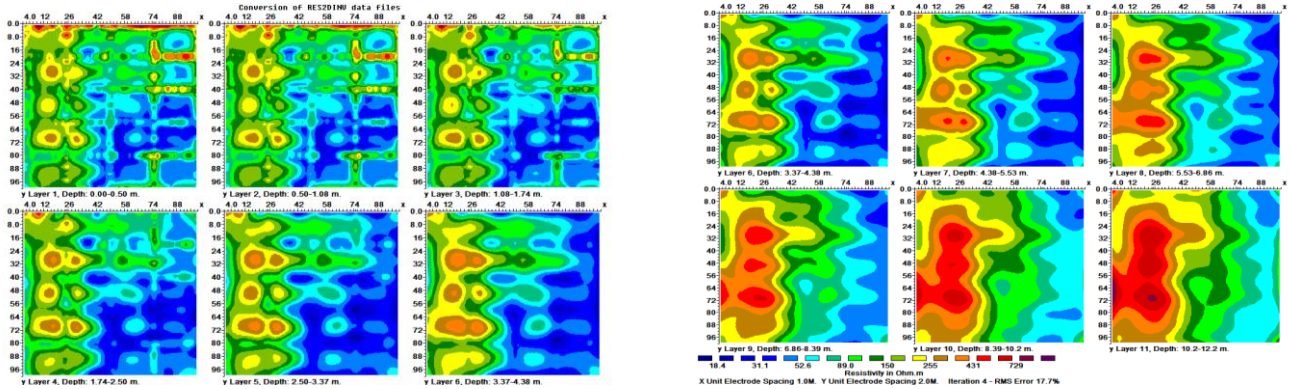

Figure 3: Horizontal depth slices of the 3D inverse model obtained from the orthogonal 2D profiles (field data).

CONCLUSIONS

The study shows that 3D geoelectrical resistivity imaging can be achieved by collating orthogonal sets of 2D profiles. Among the arrays studied, DDP, PDP, and WSC arrays are more sensitive to 3D features and produced better image resolution. The inter-line spacing of less than or equal $4a$ will yield reliable 3D inverse models. Inter-line spacing greater than $4a$ may produce more near-surface artefacts in the inverse models but can be very useful. 3D geoelectrical resistivity survey in which a set of orthogonal 2D profiles are combined would speed up field procedure and considerably reduced the time and effort involved in collecting 3D data set using square or rectangular grids.

ACKNOWLEDGMENTS

The Third World Academy of Science (TWAS), Italy and the Council of Scientific and Industrial Research (CSIR), India is gratefully acknowledged by the first author for providing the Fellowship for this study at the National Geophysical Research Institute (NGRI), Hyderabad, India.

REFERENCES

Aizebeokhai, A.P., 2010, 2D and 3D geoelectrical resistivity imaging: Theory and field design. *Scientific Research and Essays*, 5 (23), 3592-3605.

Aizebeokhai, A.P. and Olayinka, A.I., 2010, Anomaly effects of arrays for 3D geoelectrical resistivity imaging using orthogonal or parallel 2D profiles. *African Journal of Environmental Science and Technology*, 4 (7), 446-454.

Aizebeokhai, A.P., Olayinka, A.I. and Singh, V.S., 2009, Numerical evaluation of 3D geoelectrical resistivity imaging for environmental and engineering investigations using orthogonal 2D profiles, *SEG Expanded Abstracts 28*, 1440-1444.

Aizebeokhai, A.P., Olayinka, A.I. and Singh, V.S., 2010, Application of 2D and 3D geoelectrical resistivity imaging for engineering site investigation in a crystalline basement terrain, southwestern Nigeria. *Journal of Environmental Earth Sciences*, 1481-1492.

Amidu, S.A. and Olayinka, A.I., 2006, Environmental assessment of sewage disposal systems using 2D electrical resistivity imaging and geochemical analysis: A case study from Ibadan, Southwestern Nigeria. *Environment and Engineering Geoscience*, 7 (3), 261-272.

Bentley, L.R. and Gharibi, M., 2004, Two- and three-dimensional electrical resistivity imaging at a heterogeneous site. *Geophysics*, 69(3), 674-680.

Chambers, J.E., Ogilvy, R.D., Kuras, O., Cripps, J.C. and Meldrum, P.I., 2002, 3D electrical mapping of known targets at controlled environmental test site. *Environmental Geology*, 41, 690-704.

Chambers, J.E., Ogilvy, R.D., Meldrum, P.I. and Nissen, J., 1999, 3D electrical resistivity imaging of buried oil-tar contaminated waste deposits. *European Journal of Environmental and Engineering Geophysics*, 4, 3-15.

Dahlin, T. and Loke, M.H., 1998, Resolution of 2D Wenner resistivity imaging as assessed by numerical modelling. *Journal of Applied Geophysics*, 38 (4), 237-248.

de Groot-Hedlin, C. and Constable, S.C., 1990, Occam's inversion to generate smooth two-dimensional models from magnetotelluric data. *Geophysics*, 55, 1613-1624.

Dey, A. and Morrison, H.F., 1979, Resistivity modelling for arbitrary shaped two-dimensional structures. *Geophysical Prospecting*, 27, 1020-1036.

Griffiths, D.H. and Barker, R.D., 1993, Two dimensional resistivity imaging and modeling in areas of complex geology. *Journal of Applied Geophysics*, 29, 211-226.

Li, Y. and Oldenburg, D.W., 1994, Inversion of 3D DC resistivity data using an approximate inverse mapping. *Geophysical Journal International*, 116, 527-537.

Loke, M.H. and Barker, R.D., 1996a, Practical techniques for 3D resistivity surveys and data inversion. *Geophysical Prospecting*, 44, 499-524.

Loke, M.H. and Barker, R.D., 1996b, Rapid least-squares inversion of apparent resistivity pseudo-sections by a quasi-Newton method. *Geophysical Prospecting*, 44, 131-152.

Press, W.H., Teukolsky, S.A., Vetterling, W.T. and Flannery, B.P., 1996, *Numerical recipes in Fortran 77: The Art of Scientific Computing*, 2nd edn., Cambridge University Press.